Chinese Journal of Natural Medicines

Natural-derived porous nanocarriers for the delivery of essential oils

Hongxin CHEN, Xiaoyu SU, Yijuan LUO, Yan LIAO, Fengxia WANG, Lizhen HUANG, Aiguo FAN, Jing LI, Pengfei YUE

Citation: Hongxin CHEN, Xiaoyu SU, Yijuan LUO, Yan LIAO, Fengxia WANG, Lizhen HUANG, Aiguo FAN, Jing LI, Pengfei YUE, Natural-derived porous nanocarriers for the delivery of essential oils, Chinese Journal of Natural Medicines, 2024, 22(12), 1117-1133. doi: 10.1016/S1875-5364(24)60731-4.

View online: https://doi.org/10.1016/S1875-5364(24)60731-4

Available online at www.sciencedirect.com
ScienceDirect
Chinese Journal of Natural Medicines 2024, **22**(12): 1117-1133
doi: 10.1016/S1875-5364(24)60731-4
Chinese Journal of Natural Medicines
"Natural-derived drug carriers (NDDCs) for precision therapy"Special Issue
•Review•

Natural-derived porous nanocarriers for the delivery of essential oils

CHEN Hongxin[1], SU Xiaoyu[1], LUO Yijuan[1], LIAO Yan[1], WANG Fengxia[1], HUANG Lizhen[1], FAN Aiguo[1], LI Jing[4], YUE Pengfei[1, 2, 3*]

[1] *Key Laboratory of Modern Preparation of TCM, Ministry of Education, Jiangxi University of Chinese Medicine, Nanchang 330004, China;*
[2] *State Key Laboratory for the Modernization of Classical and Famous Prescriptions of Chinese Medicine, Nanchang 330096, China;*
[3] *Research and Development Department, Jiangzhong Pharmaceutical Co., Ltd., Nanchang 330004, China;*
[4] *Jiangxi Provincial Institute of Traditional Chinese Medicine, Nanchang 330077, China*

Available online 20 Dec., 2024

[ABSTRACT] Essential oils (EOs) are natural, volatile substances derived from aromatic plants. They exhibit multiple pharmacological effects, including antibacterial, anticancer, anti-inflammatory, and antioxidant properties, with broad application prospects in health care, food, and agriculture. However, the instability of volatile components, which are susceptible to deterioration under light, heat, and oxygen exposure, as well as limited water solubility, have significantly impeded the development and application of EOs. Porous nanoclays are natural clay minerals with a layered structure. They possess unique structural characteristics such as large pore size, regular distribution, and tunable particle size, which are extensively utilized in drug delivery, adsorption separation, reaction catalysis, and other fields. Natural-derived porous nanoclays have garnered considerable attention for the encapsulation and delivery of EOs. This review comprehensively summarizes the structure, types, and properties of natural-derived porous nanoclays, focusing on the structural characteristics of porous nanoclays such as montmorillonite, palygorskite, halloysite, kaolinite, vermiculite, and natural zeolite. It also examines research advances in their delivery of EOs and explores engineering strategies to enhance the delivery of EOs by natural-derived porous nanoclays. Finally, various applications of natural-derived porous nanoclays for EOs in antibacterial, food preservation, repellent, and insecticide aspects are presented, providing a reference for the development and application of EOs.

[KEY WORDS] Essential oils; Natural-derived porous nanoclays; Delivery; Engineering strategies; Application
[CLC Number] R944 **[Document code]** A **[Article ID]** 2095-6975(2024)12-1117-17

Introduction

EOs are naturally occurring secondary metabolites derived from various parts of aromatic plants. These volatile natural compounds are also referred to as volatile oils [1, 2]. EOs consist of an oily mixture with a complex chemical composition, primarily comprising volatile components such as hydrocarbons (including monoterpenes, sesquiterpenes, diterpenes, and phenylpropanoids) and oxygen-containing derivatives (including alcohols, esters, aldehydes, ketones, phenols, and ethers) [3-6]. EOs exhibit multiple pharmacological properties, including antibacterial, anti-inflammatory, anti-tumor, antioxidant, and anthelmintic activities [7-13]. The FDA has long classified EOs as GRAS (Generally Recognized as Safe) substances [14], and they have played a crucial role in medicine, cosmetics, food, and agriculture [15-19].

Nonetheless, EOs possess certain limitations that hinder their development and application, including pronounced hydrophobicity, volatility, chemical instability, and intense odor [20, 21]. These characteristics present significant challenges in the field of essential oil delivery. Currently, numerous studies report on the use of nanocarriers for EO delivery, such as mesoporous silica nanoparticles (MSNs) [22, 23], metal-organic frameworks (MOFs) [24, 25], and polymer nanoparticles (PNPs) [26, 27]. However, these nanocarriers face issues related to mass-production reproducibility and inadequate biocompatibility. Consequently, the search for suit-

[Received on] 12-Jul.-2024
[Research funding] This work was supported by the National Natural Science Foundation of China (Nos. 82474087, 82274108), the Young Qihuang Scholar Program of Traditional Chinese Medicine of the State (No. 2022256), Jiangxi University of Chinese Medicine Science and Technology Innovation Team Development Program (No. CXTD22006), and Jiangxi Province 2023 Graduate Innovation Special Fund Project (No. YC2023-S793).
[*Corresponding author] E-mail: pengfeiyue@jxutcm.edu.cn
These authors have no conflict of interest to declare.

able delivery carrier materials to address the instability of EOs remains an active area of research.

Natural-derived porous nanoclays are clay minerals with mesoporous structures occurring in nature, hailed as the materials of the "greening twenty-first-century material world". These nanoscale layered silicates [28] are chemically composed of Si, O, Al, and Mg elements. The fundamental structural units of nanoclays are silicon-oxygen tetrahedrons and aluminum (magnesium)-oxygen octahedrons, which form tetrahedral sheets (T sheets) and octahedral sheets (O sheets), respectively. These sheets are connected vertically by hydrogen bonds, creating the basic layered structure of nanoclays [29]. Based on the stacking arrangements of T and O sheets, nanoclays are primarily categorized into 1 : 1 (TO) type and 2 : 1 (TOT) type clay [30]. Natural-derived porous nanoclays exhibit diverse morphologies, including nanorods, tubes, fibers, and sheets [31]. This unique nanostructure provides an inherent structural foundation for drug delivery. Moreover, these nanoclays possess high porosity, large specific surface area, chemical and mechanical stability, and a distinct structure with varied morphologies. They find widespread applications in medical care, catalysts, agriculture, and other fields [32-34]. With excellent cation exchange capacity and adsorption properties, natural-derived porous nanoclays can adsorb EOs through hydrogen bond adsorption [35], electrostatic action [36], hydrophobic interaction [37], and other adsorption methods, thereby enhancing their stability. This approach offers a novel strategy to address the issue of insufficient stability in EOs.

Natural-derived porous materials, particularly nanoclays, have garnered significant attention in the medical field [38, 39]. A comprehensive review is essential to fully comprehend the considerable potential of nanoclays in the encapsulation and delivery of EOs. As illustrated in Fig. 1, this review thoroughly examines several representative natural-derived porous nanoclays, including montmorillonite (MMT), kaolinite (Kaol), halloysite (HS), palygorskite (Pal), vermiculite (VML), and natural zeolite (NZ), while summarizing recent research advancements in EOs delivery. Furthermore, this review briefly discusses engineering strategies to enhance EOs delivery using natural-derived porous nanoclays. Lastly, the review concisely presents applications of these nanoclays in EOs delivery for antibacterial purposes, food preservation, repellents, and insecticides.

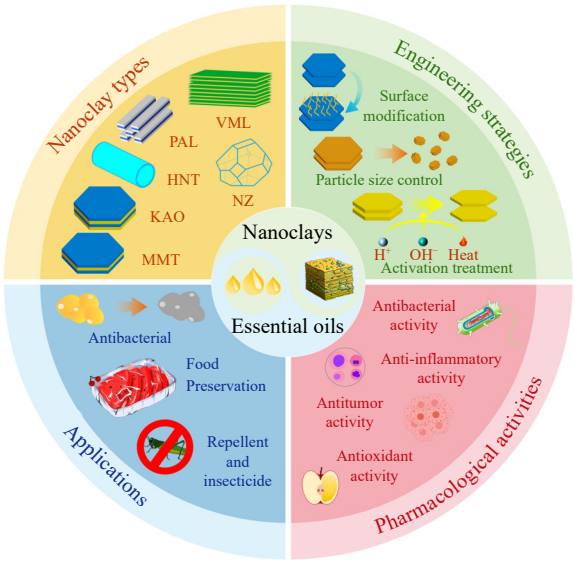

Fig. 1 Schematic diagram of natural-derived porous nanoclays as nanocarriers for EOs and the pharmacological activities of EOs.

Overview of Natural-derived Porous Nanoclays

Natural-derived porous nanoclays are layered silicate materials with a nanoscale pore structure. These materials, which exist in various forms, possess unique structural and functional properties that facilitate their widespread application. They are utilized in diverse fields, including catalysts [40], adsorbents [41], and drug carriers [42].

Structure of natural-derived porous nanoclays

The fundamental composition of porous clay materials comprises natural clay minerals. These minerals are characterized as layered silicates [43], with a structure consisting of two primary structural units: silicon-oxygen tetrahedra and aluminum-oxygen or magnesium-oxygen octahedra. The silicon-oxygen tetrahedron has Si^{4+} at its center, with O^{2-} at the four vertices. Multiple silicon-oxygen tetrahedra interconnect at their vertices to form a tetrahedral sheet with a network or chain structure, referred to as the T sheet. The octahedron's center contains Al^{3+} or Mg^{2+}, with the remaining eight vertices occupied by O^{2-} or OH^{-} [44]. Octahedra are classified as dioctahedral or trioctahedral based on their central cations. When the octahedral center contains trivalent ions such as Al^{3+} or Fe^{3+}, it is termed dioctahedral, whereas bivalent ions like Mg^{2+} or Fe^{2+} result in trioctahedral structures. Multiple octahedra arranged equidistantly form a layered structure known as the O sheet. The structural unit layer of clay minerals, also called the crystal layer, is formed when oxygen atoms from the T layer and hydroxyl groups from the O layer connect *via* hydrogen bonds [45]. This crystal layer represents the fundamental layered structure of clay minerals.

Clay minerals exhibit diverse stacking modes of T and O layers in their structural units [46]. These are primarily categorized into two types: ①1 : 1 (TO), which includes Kaol, HS, and pyrophyllite [47, 48], and ②2 : 1 (TOT), encompassing common clay minerals such as MMT, Sep, and Pal [49-51]. Typically, 1 : 1 and 2 : 1 structures maintain electrical neutrality, with T and O layers interconnected by van der Waals forces. However, the substitution of central atoms in T and O layers by lower valence cations can impact the TOT structure, particularly when trivalent cations in O layers are replaced by divalent ones. The resulting negative charges require compensation by cations in the interlayer domain [52]. This interlayer domain, a highly variable and expandable region between upper and lower structural unit layers, is generally occupied by H^{+} and various alkaline cations (Na^{+}, K^{+}, Mg^{2+},

and Ca^{2+}). The characteristics of the interlayer domain significantly influence the physical and chemical properties of clay minerals, including their adsorption capacity, expansibility, and cation exchange capacity.

Types of natural-derived porous nanoclays

Currently, approximately 30 types of clay materials exist, each with distinct mineralogical compositions, structural morphologies, and physicochemical properties [53]. Clay materials are categorized based on the stacking arrangement of their structural units into two primary types: 1 : 1 (TO) and 2 : 1 (TOT). Further classification is based on variations in the clay material interlayer and the negative charge X per unit cell (Table 1).

1 : 1 (TO) clay minerals, including Kaol, HS, lizardite, and chrysotile, lack interlayers or contain only H_2O, with X = 0. These clays exhibit stable physical and chemical properties, high molecular stability, and limited or non-existent isomorphic substitution [54]. In 2 : 1 (TOT) clays, talc, willemseite, and pyrophyllite lack intercalation, while Sep and palygorskite contain only H_2O. The negative charge X per unit cell for these clays is 0. Smectite and VML, both containing hydrated cations, demonstrate good expansion properties. Smectite, including MMT, beidellite, and saponite, has an X range of 0.2 to 0.6, while VML's X ranges from 0.6 to 0.9, categorized as trioctahedral or dioctahedral. Non-expansive clays with non-hydrated cationic interlayers are classified as micas. When X ranges from 0.5 to 1.0, illite, glauconite, muscovite, and paragonite are considered mica clays. Chlorite clays have hydroxide interlayers with an uncertain X range and include varieties such as chlorite, clinochlore, and donbassite [55].

Natural-derived Porous Nanoclays as Nanocarriers of EOs

MMT

MMT is a clay material belonging to the smectite subgroup. Its general formula is $(Ca, Na)_{0.33}(Al, Mg)_2(Si_4O_{10})(OH)_2 \cdot nH_2O$ [56]. MMT is a member of the highly expansive three-layer (TOT) layered silicate family, with particle sizes ranging from 1-2 μm, classifying it as a typical 2 : 1 layered clay [57]. The fundamental structure of MMT comprises an aluminum oxide dioctahedral layer sandwiched between two silicon oxide tetrahedron layers. These structural unit layers are held together by van der Waals forces, with an interlayer spacing of 1.2–1.6 nm. Si^{4+} in the T layer and Al^{3+} in the O layer are susceptible to replacement by lower-valent cations, resulting in a permanent negative charge in the MMT interlayer. Post isomorphic substitution, the negative charge per unit cell of the interlayer ranges between 0.2 and 0.6 [58, 59]. These structural characteristics endow MMT with advantageous properties, such as excellent cation exchange capacity, high expansibility, large specific surface area, and ease of surface structure modification [49]. These attributes form the basis for the production of various MMT derivative materials and create favorable conditions for the adsorption of EOs. However, unmodified MMT nanoclays still present limitations in EO delivery, including suboptimal loading efficiency, inadequate control over release kinetics, and potential adverse effects on the pharmacological activity of the entrapped compounds [60].

MMT clay materials, modified from MMT clay minerals, have been widely used to enhance the stability of EOs. Kamal *et al.* [61] investigated the adsorption-release dynamics of thyme oil, thymol, and carvacrol (CRV) on sodium MMT (Na^+-Mt) and simulated the adsorption mechanism of thymol on Na^+-Mt. All three components demonstrated effective adsorption onto Na^+-Mt. Simulation results indicated that the −OH group of thymol forms intermolecular hydrogen bonds with the −OH on the Na^+-Mt surface, facilitating thymol adsorption on the outer surface of Na^+-Mt. Gas chromatography detection revealed that active ingredients of thyme EO were still detectable after 24 days of release. The study demonstrated that Na^+-Mt adsorption played a significant role in controlling the release process and mitigating environmental effects on thyme oil and its volatile components. In addition to metal ion modifications, cationic surfactants with long carbon chain structures are commonly employed as MMT modifiers. Jn *et al.* [62] proposed an interaction scheme

Table 1 Main types of porous clay materials.

Layer stacking	Interlayer	X	Clay mineral group	Clay mineral name
1 : 1	None or only H_2O	0	Kaolin	Kaol, HS, Dickite
			Serpentine	Chrysotile, Lizardite, Antigorite
2 : 1	None	0	Talc	Talc, Willemseite
			Pyrophyllite	Pyrophyllite, Ferripyrophyllite
	Only H_2O	0	Sep	Sep
			Paligorskite	Paligorskite
	Hidrated cations	0.2–0.6	Smectite	MMT, Beidellite, Saponite
		0.6–0.9	VML	Dioctahedral VML, Trioctahedral VML
	Non-hydrated cations	0.5–1.0	Mica	Ilite, Moscovite, Glauconite, Biotite, Paragonite
	Hydroxide	Variable	Chlorite	Clinochlore, Donbassite, Sudoite, Cookeite

between volatile oils and modified MMT and porous HNT clay (Table 2). A multilayer thin film reservoir of clay/volatile oils composite was prepared using octadecyl-modified MMT nanoclays to adsorb orange and thyme oils. Results indicated that volatile oils increased the interlayer spacing of MMT by approximately 10%, with MMT clay exhibiting a more pronounced increase. MMT demonstrated higher adsorption rates and better interaction with thyme oil compared to orange oil; MMT/thyme oil embedded in multilayer film with a thinner polyamide (PA-6) layer showed maximum cymene release of 800 μg after 72 hours. This film material offers potential as a controlled-release system for EOs, with applications in pest management and food packaging industries. Furthermore, modifying MMT with cationic surfactants can alter the clay's crystal structure and enhance its adsorption capacity. Nguemtchouin *et al.* [63] utilized MMT clay materials, both in their native state and after modification with hexadecyltrimethylammonium CTMA, to adsorb *Ocimum gratissimum* EO. These treated clay materials were subsequently employed in insecticidal assays against *Sitophilus zeamais*, a maize pest. Experimental findings revealed that unmodified composite clay materials exhibited minimal insecticidal potency, losing all activity after 30 days. Conversely, modified MMT composite clay materials retained approximately 40% of their initial insecticidal effectiveness after 30 days, demonstrating enhanced capacity to induce insect mortality and sustained insecticidal performance. This improvement was attributed to CTMA-modified MMT adsorbing more insecticidal active ingredients. In conclusion, montmorillonite modification presents an effective method for improving EO stabilization and expanding the application range of MMT.

Kaol

Kaol is a layered silicate mineral with a 1 : 1 TO structure, belonging to the Kaol family of clay minerals. Its general formula is $Al_2Si_2O_5(OH)_4$ [64]. As one of the most abundant clay minerals on Earth, Kaol finds extensive applications in medicine, food additives, chemical fertilizers, cosmetics, and other industries [65, 66]. The fundamental structural unit of Kaol comprises a silicon-oxygen tetrahedral layer bonded to an aluminum-oxygen dioctahedral layer. The siloxane base of this unit exhibits a partial negative charge, while the aluminum alcohol base carries a partial positive charge. Driven by dipole properties, the siloxane surface forms a dense network of interlayer hydrogen bonds and strong dipole interactions with the aluminum alcohol surface, resulting in a book-like structure with particle sizes ranging from 200 nm to 1 μm. This compact structure imparts stable physical and chemical properties to Kaol [67-69]. The basic layers of Kaol are tightly bound by hydrogen bonds, with no interlayer or only H_2O present. The negative charge per unit cell (X) is 0, contributing to high molecular stability. Isomorphic substitution is limited or non-existent, resulting in a low cation exchange capacity of only 1−6 meq·100g^{-1} for Kaol [54, 70]. Despite these characteristics, Kaol presents several challenges, including limited dispersibility, lack of selectivity in drug loading, and larger particle size [71]. However, these limitations can be substantially mitigated through surface modification and functionalization techniques, thereby enhancing Kaol's potential application in EO delivery systems [72, 73].

Kaol exhibits exceptional physical, chemical, and surface properties. Due to the interaction between its surface and organic matter, Kaol and its modified derivatives serve as effective carriers for EOs [74]. Mahdi *et al.* [75] utilized Kaol as a mineral carrier, incorporating LEO into Kaol *via* vacuum pulling method, and subsequently added the Kaol-LEO complex into LDPE through melt compounding to produce active composite films. The study examined the thermal stability, antibacterial properties, and limonene release of the LDPE composite membrane. Thermogravimetric analysis (TGA) results indicated that the LEO content remained consistent at 20%−25% during the processes of LEO loading and melt film formation. The use of Kaol as a carrier and the film preparation method significantly enhanced the thermal stability of LEO and slowed the release of limonene. The antibacterial properties of the LEO-containing film against *Escherichia coli* were investigated. The findings demonstrate that the novel active composite exhibits significant antibacterial activity, suggesting considerable potential for active packaging applications. Costa *et al.* [76] developed poly(hydroxybutyrate-hydroxyvalerate) (PHBV) nanocomposite films through a melting process, combining Kaol, OEO as an antibacterial agent, and PHBV. The release study revealed that the PHBV/Kaol/OEO film's release profile initially showed rapid release of surface-bound OEO, followed by sustained release in the intermediate and later stages. During a 48-hour release experiment, the PHBV/Kaol/OEO film released 20.8% ± 2.7% of OEO. This biphasic release pattern provides an initial burst of antimicrobial active ingredients, potentially reducing pathogenic bacterial populations during food storage, followed by sustained release of active compounds for prolonged inhibition of bacterial growth.

HS

HS, a member of the kaolin group alongside Kaol, is a hydrated polytypic clay with the general formula $Al_2Si_2O_5(OH)_4{\cdot}nH_2O$. It is characterized by a dioctahedral 1 : 1 TO structure, with its structural unit layer comprising a silicon-oxygen tetrahedron layer and an aluminum-oxygen dioctahedron layer. The interlayer of the structural unit consists of water molecules, and each unit cell has a negative charge X of 0. HS exhibits hollow tubular, spherical, and lamellar morphologies, with halloysite nanotubes (HNTs) being the most prevalent structure in nature [77]. HNTs possess a unique porous hollow tubular structure, distinguishing them from other clay materials. Their dimensions typically range from 40−70 nm in external diameter, 10−40 nm in inner diameter, and 0.2−2.0 μm in tube length [78]. The structure of HNTs consists of an octahedral gibbsite sheet (Al-OH) on the inner surface, a layer of siloxane sheets (Si-O-Si) on the out-

Table 2 The cases and application of natural-derived porous nanoclays for delivery of EOs

Clay material	EOs/EOs components	Pore parameters	Performance	Application	Target organism	Ref
MMT and HNT	Orange oil and Thyme oil	The interlayer spacing (d001) of MMT is 2.2 nm. The diameter and length of HNT are 30–70 nm and 1–3 μm.	The clay/EO composite showed a long-term continuous release of EO.	-	-	[62]
Na^+-Mt	Thyme oil, thymol, and CRV	The specific surface S_{BET} and total pore volume V_t of Na^+-Mt are 83.49 $m^2 \cdot g^{-1}$ and 0.213 $cm^3 \cdot g^{-1}$.	Prolonging the release time of active molecules adsorbed by Na^+-Mt and protecting them from the influence of the environment.	-	-	[61]
Mont-CTMA	*Ocimum gratissimum* EO	-	The insecticidal effect of *Ocimum gratissimum* EO was extended from 7 days to 80 days.	Insecticide	Insect: beetles	[63]
MMTNa and MMTCa	Rosemary EO (REO) and ginger EO (GEO)	A high surface area (700–800 $m^2 \cdot g^{-1}$) and a thickness of approximately 1 nm.	Enhance antioxidant effect, reduce 6%–16% microbial contamination, and extend the shelf life of fresh poultry meat.	Active packaging	Total coliforms	[128]
Mt	Citronellol (Col), citral (Cal) and linalool (Lol)	Total specific surface area (TSSA) = 621 $m^2 \cdot g^{-1}$	Showing higher antifungal activity.	Antifungal coating	*Chaetomium globosum*, *Alternaria alternata* and *Aspergillus fumigatus*	[35]
MMT	*Carum copticum* EOs	Moisture content between 2% and 5%, particle size of 20–30 nm	Delay the oxidation and microbial corruption of local butter	Active films for food packaging (butter)	*Bacillus cereus* and *Escherichia coli*	[49]
HNTs	LEO	HNTs: The specific surface area, diameter, and length are 50.8 $m^2 \cdot g^{-1}$, 30–70 nm and 1–3 μm.	The initial limonene content of 20-25% is not affected by thermal degradation and limonene can be continuously released from LDPE film.	Active packaging	*Escherichia coli*	[75]
Kaol, Hal and Sep	OEO	-	The sustained release process of OEO from clay particles was realized.	Antimicrobial active food packaging	*Escherichia coli* and *Staphylococcus aureus*	[76]
HNTs and N-HNTs	Thyme oil	The length of HNTs is about 500-1000 nm. The inner diameter of N-HNT increased from 5–15 nm to 15–25 nm.	The sustained release of thyme oil from HNT can last for up to 21 days.	Antimicrobial Packaging	*Escherichia coli*, molds, and yeasts	[84]
Hal	Cinnamaldehyde	The length of Hal is about 1 μm, and the diameter is approximately 50–100 nm.	It improves the thermal stability of cinnamaldehyde, and makes it slowly release into water.	Conservation of stone cultural heritage	*Bacillus subtilis* and *Aspergillus niger*	[85]
HNTs	CA	The length of HNTs is 1000–1500 nm, and the outer diameter range is 50–70 nm.	After 25 days of long-term storage at 40 °C, CA was slowly released, with a release rate of 33.8 %.	Antibacterial packaging	*Escherichia coli* and *Staphylococcus aureus*	[86]

Continued

Clay material	EOs/EOs components	Pore parameters	Performance	Application	Target organism	Ref
HNTs	Peppermint EO	-	The release behavior of PO in 50% ethanol solution is thermosensitive.	Food packaging	*Escherichia coli* and *Staphylococcus aureus*	[129]
Sep	Rosemary EO	The cation exchange capacity (CEC) and specific surface area (SSA) of Sep are 0.15 $mmole_c \cdot g^{-1}$ and 340 $m^2 \cdot g^{-1}$.	The phytotoxicity of ROEO was reduced.	Insecticide	Insect: thrips	[130]
Hal	*Rosa damascena* EO	The Hal has a diameter of 30–70 nm and length of 1–3 μm.	Hal plays a role in thermal insulation and delays the migration of EO molecules from the matrix.	Food packaging	*Escherichia coli* and *Staphylococcus aureus*	[131]
HNTs and A-HNTs	Cinnamaldehyde（Cin）	After acid treatment, the surface area of A-HNT increased from 50.30–80.17 $m^2 \cdot g^{-1}$, and the pore volume increased from 0.25–0.33 $m^3 \cdot g^{-1}$.	The 14-day cumulative release rate of Cin was about 60%, and the slow release of Cin was realized.	Antibacterial packaging film	*Escherichia coli* and *Staphylococcus aureus*	[87]
Pal	Tea tree oil（TTO）	The length of Pal is 170–600 nm, and the width is 15–25 nm.	TTO loading on Pal can produce excessive MDA and ROS, leading to bacterial death.	Antibacterial	*Escherichia coli*, *Staphylococcus aureus*, *propionibacterium acnes*, and *Staphylococcus epidermidis*	[132]
APT	CRV	The original APT is a typical rod-like morphology with a diameter of 10–30 nm and a length of 0.5–2 μm.	The nanocomposites showed good antibacterial properties, and the MIC values for *S.aureus* and *E.coli* were both 2.0 $mg \cdot mL^{-1}$.	Antibacterial	*Escherichia coli* and *Staphylococcus aureus*	[97]
PGS	Ginger EO (GEO)	-	GEO-PGS improves the thermal stability of GEO.	Antibacterial	*Escherichia coli* and *Staphylococcus aureus*	[98]
VML	LEO	-	At 4 °C, the cumulative release rate of 80 h was 68 %, and the slow and continuous release of LEO was realized.	Food preservation	*Escherichia coli*	[112]
VML	OEO	VML particle size in the range of 200−1000 nm	Within 14 h, 45.31% of OEO was continuously released from VML at constant temperature (60 °C).	Antibacterial	*Escherichia coli* and *Staphylococcus epidermidis*	[113]
NZ	CEO	-	Increase the insecticidal effect of CEO from 1 day to 10 days	Insecticide	*P. operculella*	[127]
Zeolite	OEO	-	The thermal stability of OEO was improved by curing OEO.	-	-	[126]
ZEO	*Ruta graveolens* EO (RGEO)	-	RGEO was gradually released from the pores of ZEO and lasted for 90 days.	Insecticide	*Sitophilus zeamais* (L.)	[125]

er surface, and water in the middle layer interacting with the inner surface group Al-OH [79]. Notably, HNTs exhibit differential charge characteristics over a wide pH range, with the outer surface carrying a negative charge and the inner surface a positive charge [80]. The distinctive porous hollow structure of HNTs enhances their adsorption properties, allowing for the encapsulation of active ingredients within the nanotube cavity and reducing their release rate [62, 81]. HNTs offer advantages such as a unique tubular structure, low cytotoxicity, and the potential for functionalization of both internal and external surfaces [82]. Consequently, HNTs find widespread application in drug loading and sustained release, nanocomposites, environmental pollution control, and food industries. However, it is important to note that the strong adsorption capacity of HNTs poses challenges in precisely controlling release rates. Additionally, the *in vivo* behavior of HNTs remains to be fully elucidated, and their biodegradation is known to be problematic [83].

Numerous studies have demonstrated the efficacy of HNTs as carriers for traditional Chinese medicine EOs, enhancing their thermal stability, prolonging their action time, and achieving controlled release [75, 84-88]. Oliveira *et al.* [88] modified Hal and Kaol with OEO using a method for modifying nanoclay particles with EOs. OEO was adsorbed on the outer surface and inner cavity of the clay. At a clay : EO ratio of 10 : 1, Hal : 10-OEO exhibited the highest oil loading rate (45%), surpassing that of Kaol (43%). Evaporation assay results at 25 °C revealed that pure OEO evaporated significantly faster than the nanocomposite formulation. The pore structure and hydrogen bonding of Hal and Kaol facilitated the slow release of OEO. Hal : 10-OEO demonstrated lower OEO evaporation compared to Kaol : 10-OEO, indicating superior OEO retention by Hal. This was attributed to Hal's larger inner cavity and specific surface area, allowing for increased OEO-Hal surface interactions and reduced OEO volatility. Wang *et al*. [85] developed a sustained release system based on HNTs by loading cinnamaldehyde (Cin) into acid-activated HNT (Hal-4M) using a vacuum method. They investigated the release characteristics of Cin and Cin-Hal-4M in distilled water. Results showed that pure Cin exhibited burst release, with a 95% cumulative release rate within 3 days. Cin-Hal-4M demonstrated initial burst release on day 1, followed by a slow release process from day 2−10, with a Fickian diffusion release mechanism. Field tests on stone statues using this sustained release system showed a 79% decrease in ATP levels (a sensitive indicator of microbial presence) in the Cin-Hal-4M treatment area after one year, confirming its effectiveness. Zheng *et al*. [86] selected carvanol (CA) as an antimicrobial agent and loaded it into acid-treated HNTs *via* vacuum suction. Release studies at various temperatures revealed that the cumulative release rate of CA from CA-HNTs was significantly lower than that of pure CA within 25 days. After 25 days of storage at 40 °C, the cumulative release rate of CA from CA-HNTs decreased markedly to 33.4%, compared to 38.4% for pure CA. These results demonstrate the potential for sustained release of CA through CA-HNT interactions.

Pal

Pal, also known as attapulgite (APT), with the chemical formula $(Mg, Al)_2Si_4O_{10}(OH)\cdot 4H_2O$, is a one-dimensional nano-sized hydrated magnesium aluminosilicate clay mineral with a 2 : 1 TOT structure, exhibiting a nanorod-like crystal form, uniform nano-pore size, and active surface silanol groups [51, 89]. The structural unit layer of Pal is chain-like, containing interlayer water molecules, with a cation exchange capacity (CEC) between 30−40 meq·100g^{-1}. Each structural unit sheet comprises two opposing T sheets connected to each other, with O sheets stacked between them, resulting in a unique crystal structure featuring zeolite channels (0.37 × 0.64 nm^2) and active silanol groups [90, 91]. Its distinctive crystal structure, fibrous morphology, and nanometer size imbue Pal with high porosity, large specific surface area, and numerous active sites for molecular interactions [92]. Consequently, Pal finds widespread application in drug delivery systems, wastewater treatment, modern agriculture, and construction materials [93-96].

The regular pores and silane alcohol active groups on palygorskite clay's surface provide conditions for PAL to interact with EOs and enhance its stability. Zhong *et al.* [97] utilized APT as a carrier to successfully prepare a composite nano-antibacterial material. This was achieved by mechanically grinding CAR molecules to replace zeolite water molecules in the APT pores, subsequently loading them inside. This illustrates that the potential interaction mechanism between APT and CAR/APT-30 was prepared with 30 wt% CRV content and 30 min grinding time. The antimicrobial properties of CAR/APT-30 against *Staphylococcus aureus* and *Escherichia coli* were investigated. The MIC of CAR/APT-30 against both bacteria was 2 mg·mL^{-1}, demonstrating strong antibacterial performance. Lei *et al.* [98] developed a novel antibacterial composite clay material (GEO-PGS) with good stability by loading GEO into PGS *via* ion exchange, using PGS as the drug carrier. TG results confirmed the interaction between GEO and PGS, indicating successful adsorption of GEO on the PGS surface. The oil loading rate of GEO in the composite clay material was approximately 18.66%. The *in vitro* antibacterial test of GEO-PGS revealed poor antibacterial activity of PGS alone. However, due to PGS's bacterial adsorption ability, GEO-PGS adsorbed onto the bacterial surface, allowing GEO to fully contact bacteria and exert a significant antibacterial effect. The MIC of GEO against *Staphylococcus aureus* was 6.25 mg·mL^{-1}. After calcination at 121 and 200 °C, the MIC value of GEO-PGS remained at 6.25 mg·mL^{-1}, indicating good thermal stability and persistent strong antibacterial activity. In conclusion, while Pal demonstrates potential in EOs delivery systems, its fibrous structure's intrinsic shape limits the actual drug loading space, consequently restricting Pal's drug loading capacity. Furthermore, Pal exhibits poor dispersion and biocompatibility [99, 100].

VML

VML is a two-dimensional layered silicate belonging to the hydromica family, with a theoretical formula of (Mg, Fe, Al)$_8$(Si, Al)$_4$O$_{10}$(OH)$_2$·4H$_2$O and a basic structure of 2 : 1 TOT [101, 102]. Similar to MMT, VML is a highly expansive clay material with an interlayer spacing of approximately 1.4 nm. Its interlayer domain contains numerous hydrated cations, predominantly Mg^{2+} [103]. The negative charge X per unit cell of VML ranges from 0.6 to 0.9. During homogeneous substitution, Si^{4+} in the silicon-oxygen tetrahedron is replaced by Al^{3+}, while Mg^{2+} in the magnesia octahedron is substituted by lower valence ions such as Li^{+}, resulting in a permanent negative charge in the interlayer domain. These negative charges are neutralized by metal cations between layers [102, 104]. As a commonly utilized nanoclay material, VML exhibits strong adsorption capacity, excellent expansibility, good biocompatibility, and high cation exchange capacity [105, 106]. Consequently, it finds widespread applications in sewage treatment, adsorption separation, drug delivery, and other fields [107-110].

Two-dimensional layered VML is a nanoclays material with significant potential for delivering EOs. It exhibits excellent adsorption properties, a large specific surface area, and a rich porous structure [111]. Li *et al.* [112] incorporated LEO into porous layered VML and combined it with KGM-g-PAA/PVA composites to develop composite antibacterial water absorption pads. Their research revealed that the VML dosage substantially impacted the release of LEO in the composite antibacterial absorbent pad. PVA composites to prepare composite antibacterial water absorption pads. Li *et al*. found that the dosage of VML significantly influenced the release of LEO in the composite antibacterial absorbent pad. depicts the release curve of LEO at VML dosages of 0, 0.5, 1, and 1.5. The cumulative release rate of LEO in the antibacterial absorbent pad without VML rapidly increased to 78% (50 h), indicating an inability to achieve sustained LEO release. Conversely, at a VML dosage of 1.5 g, the cumulative LEO release rate over 76 h decreased to 48.6%, attributed to excessive VML reducing the interlayer gap and increasing LEO's migration resistance. These findings suggest that VML could effectively regulate LEO release, mitigate its volatilization, and preserve its active components. Kothalawala *et al*. [113] employed a simple mechanical mixing method to incorporate OEO into the pores of SMV particles. TGA indicated an OEO loading efficiency of 5.27%. presents the release curves of free OEO, SMV, and SMV loaded with OEO at a constant temperature of 60 °C for 14 hours. The weight loss percentages for SMV and SMV loaded with OEO were 3.61% and 5.79%, respectively, while free OEO completely dissipated after 11 h. Based on the weight loss, it was calculated that 45.31% of OEO loaded in SMV was released at a constant temperature of 60 °C over 14 h. These results demonstrate that SMV enhanced the thermal stability of OEO and facilitated controlled release under constant temperature conditions. While utilizing VML as a carrier for EOs offers certain advantages, it also presents challenges, including irreversible adsorption, potential loss of EO components, and inconsistent particle size distribution [114].

NZs

NZs are hydrated crystalline aluminosilicates with a molecular formula of $M_{x/n}[(AlO_2)_x(SiO_2)_y]\cdot nH_2O$ [115, 116]. These crystalline inorganic polymers consist of TO_4 tetrahedrons (T: Al or Si) [115, 117]. The fundamental framework of NZs is characterized by a three-dimensional honeycomb structure, formed by SiO_4 and AlO_4 tetrahedrons interconnected *via* oxygen atoms, extending infinitely [118]. This structure creates channels within the zeolite, which contain water, alkali metals, and alkaline earth metal cations (such as Ca^{2+}, Na^{+}, K^{+}) [119]. When Si^{4+} in the SiO_4 tetrahedron is replaced by Al^{3+}, the resulting AlO_4 tetrahedron becomes negatively charged. To maintain overall neutrality, this charge is balanced by cations external to the NZ framework [120]. These fundamental tetrahedrons are termed primary building units (PBUs), forming the basis of the NZs framework. The geometric arrangement of PBUs is referred to as secondary building units (SBUs) [121]. The diverse types of zeolite structures are determined by the various ways in which SBUs connect to form polyhedrons. There are seven groups of SBUs and approximately 40 NZs, with clinoptilolite, chabazite, mordenite, erionite, ferromagnetite, analcime, and phillipsite being the most commonly utilized [122].

NZs possess a porous structure, high cation exchange capacity, significant adsorption capacity, and good biocompatibility, making them promising carrier materials in drug delivery applications [123, 124]. Perera *et al*.[125] developed a biocomposite material by loading RGEO into the pores of ZEO. The illustrates the FTIR spectra of RGEO, ZEO, and RGEO-ZEO bio-composites. The spectrum of the RGEO-ZEO biocomposite material exhibited an additional band of EO organic compounds at 0 days, confirming the successful incorporation of RGEO into ZEO. Over time, the relative intensity of RGEO's characteristic peaks gradually decreased after 15, 30, 60, and 90 days, indicating a sustained release of RGEO from ZEO pores over 90 days, thus addressing the volatility limitation of EOs. Migone *et al*.[126] adsorbed OEO onto ZEO and mixed it with hydroxypropyl methylcellulose (HPMC) to prepare granules, which were subsequently compressed and coated with Eudragit® EPO to produce a controlled-release tablet. This tablet effectively solidified the volatile oil and enhanced its stability against degradation and volatilization. Milićević *et al.* [127] developed an eco-friendly biological pesticide using zeolite clay materials. They encapsulated clove EO (CEO) into an emulsion (F-CNZ) using NZ (ZEOMEDIC). When insects were exposed to F-CNZ at 40 μL·L^{-1} concentration, the mortality rate decreased from 100% in 24 hours to 50% after 4 days. Compared to pure CEO's 24-hour efficacy, F-CNZ demonstrated a continuous insecticidal effect for up to 10 days, showcasing improved and prolonged CEO efficacy. While NZs serve as effective porous nanocarriers for EO encapsulation, they have limitations, including restricted adsorption selectivity and capacity and susceptibil-

ity to acid and alkali [115].

Engineering Strategies for Improving the Delivery of EOs by Natural-derived Porous nanoclays

As volatile hydrophobic natural compounds, EOs are insoluble in water and easily volatilized and degraded by environmental factors such as light, heat, and oxygen. This susceptibility hinders the efficacy of EOs' active ingredients and leads to significant loss [133-135]. To address the limitations posed by the strong hydrophobicity of EOs and enhance their stability, natural-derived porous nanoclays show considerable promise as carrier materials. These nanoclays offer advantages, including abundant availability, low cost, excellent ion exchange performance, and unique surface structural characteristics [45, 136]. However, natural-derived porous nanoclays also present certain drawbacks, such as low purity, limited porosity, and strong hydrophilicity [137]. Consequently, to enhance the encapsulation and delivery capabilities of natural-derived porous nanoclays for EOs, it is crucial to modify their surface, control their particle size, and/or activate them.

Surface modification

Natural-derived porous nanoclays possess high specific surface area, surface reactivity, and excellent ion exchange capacity. Their surface properties, including hydrophilicity, acidity, and surface charge, can be altered through surface modification. Functionalization of clay material surfaces with specific groups enhances the adsorption and release of EOs [135, 138]. Common modifiers currently in use include cationic surfactants (hexadecyltrimethylammonium bromide [139], benzyldimethylhexadecylammonium chloride [140]), polymers (polyaniline [141], chitosan [CH] [142], polydopamine [PDA] [143], polylactic acid [PLA]) and metal compounds (copper [144], sodium [145], vanadium [146][147]). Polymer surface modification is considered one of the most effective methods, attributed to the rich functional groups of polymers that can functionalize nanoclay surfaces in various ways [148]. The two primary methods for polymer modification of natural-derived porous nanoclay surfaces are physical adsorption and chemical grafting of functional polymers [148].

Proença *et al.* [147] initially combined MMT (clay), glycerol (G), and tea tree (TT) EO to prepare various samples *via* ultrasonication. Subsequently, they adsorbed PLA onto the MMT surface through melt intercalation, producing polymer-clay bionanocomposite films suitable for wound dressings using ultrasonic samples. The TGA results indicated that the mass loss of TT EO's volatile components occurred between 35 and 120 °C, with two maximum weight loss rates at 77.2 °C and 105.79 °C, respectively. The TGA results for the nanocomposite samples containing only TT EO (PLA/Clay/10TT and PLA/Clay/20TT) revealed maximum mass loss stages at 356.51 °C and 376.76 °C. These findings suggest that the modification of MMT by PLA provides barrier protection, thereby enhancing the thermal stability of TT EO.

In addition to providing protection for EOs, polymer modification can also functionally alter the surface of nanoclays to achieve intelligent controlled release of EOs. Taş *et al.* [143] developed an environmentally friendly, sunlight-triggered intelligent controlled release system (HNT-PDA/CRV-LA) utilizing HNT, PDA, LA, and CRV. The surface functionalization of HNT with PDA and LA relies on sunlight irradiation to provide heat for the photothermal material PDA, triggering the melting of the thermosensitive material LA and subsequently releasing crv. The evaporation enthalpy of CRV in the nanohybrid at each time point was tracked by DSC analysis to obtain the cumulative release curve of CRV in the absence and presence of sunlight. Within 60 days without sunlight irradiation, both HNT-PDA/crv-LA and HNT/crv-LA nanohybrids released only 40%−50% of CRV. During five cycles of sunlight irradiation, the release curve of HNT-PDA/crv-LA demonstrated the controlled release behavior of crv, with 92% of CRV molecules cumulatively released within 100 h. These results indicate that the surface modification of HNT by PDA and LA successfully achieved the intelligent controlled release of EOs.

Particle size control

Naturally occurring clay minerals typically possess large particle structures that require reduction to nanoscale dimensions to fully exploit the benefits of nanomaterials. However, these nano-sized clay units tend to aggregate, forming bulk clusters and crystal bundles. Mechanical processing can effectively disperse these large aggregates into smaller units, resulting in increased specific surface area, abundant surface groups, and enhanced interfacial compatibility [138]. While traditional mechanical treatments such as ball milling or grinding are common, ultrasonic dispersion has emerged as a novel and effective technique for particle size reduction and control.

Upasani *et al.*[149] employed ultrasonic dispersion to reduce palygorskite particle size. They utilized the response surface method to determine optimal ultrasonic conditions: 45-minute treatment time, 110 W power, 90% duty cycle, and 0.06 g·mL^{-1} clay loading. These conditions reduced palygorskite particle size to 1/16 of its initial value, significantly decreasing clay material particle size without compromising the clay crystal structure. Xu *et al.* [150] utilized industrial ultrasonic technology to depolymerize dioctahedral PAL crystal bundles. After the acid activation of palygorskite (PPal), they compared the stability of PE prepared with PPal particles under various depolymerization conditions and original palygorskite (RPal) as stabilizer, using CAR as the oil phase. Different Pal particles were dispersed in sodium alginate (SA) solution to prepare 0.5 wt% SA aqueous solution, and 10.0 wt% CAR was added to create PEs. PE stability was evaluated by measuring PE volume after 270 days. The RPal/CAR emulsion exhibited severe stratification, with an emulsion volume of only about 12.6 mL, while the emulsion volumes of PPal-30-12/CAR and PPal-50/70-8/CAR after depolymerization remained almost unchanged at 49.5 mL. After 270 days of storage, the PPal-30-12/CAR and PPal-50/70-8/CAR emulsions maintained high stability. This stability is attributed to

the extensive specific surface area and diffusion coefficient of the highly dispersed Pal nanorods, enabling quicker and firmer adsorption at the oil-water interface and lowering interfacial tension, resulting in tight encapsulation of CAR droplets [151]. These findings suggest that nanoclays with smaller particle sizes post-depolymerization offer advantages in transporting EOs.

Activation treatment

Clay activation encompasses the physical and/or chemical modification of natural-derived clay materials to optimize their performance. In numerous applications of natural-derived porous nanoclays, various activation treatments are essential [152]. Prevalent activation methods include acid [153], alkali [154], thermal, or mechanical [155] treatments, applied individually or in combination.

Traditionally, natural-derived porous clay undergoes gentle treatment with inorganic acid solutions, such as hydrochloric acid, sulfuric acid, or phosphoric acid. At a specific acid concentration, undesirable impurities like carbonates, sulfates, or oxides in clay materials can be eliminated, and the internal space of the crystal can be expanded, thereby enhancing the specific surface area, pore size, and porosity [51]. Zheng *et al.* [86] treated HNTs in a 10 wt% sulfuric acid solution and utilized them to load CRV. Transmission electron microscopy results revealed that compared to the untreated HNTs, shadows appear on the tube axis of the sulfuric acid-treated HNTs. This may be attributed to sulfuric acid reacting with the aluminate inside the nanotubes and removing it, thus widening the internal channels of the HNTs. According to the thermogravimetric (TG) results, the loading efficiency of CA on HNTs was 16%, significantly higher than previous research findings. This improvement may be due to the enlarged inner diameter of HNTs after acid activation, and the presence of numerous tiny pores between the layers, which facilitates the adsorption of a substantial amount of CA onto the nanotubes. Boro *et al.* [156] employed a 5 mol·L^{-1} sodium hydroxide solution to alkaline activate HNT, obtaining NHNT, and subsequently added a 1wt% NHNT solution to a mixed solution of PLA and CEO, preparing PLA/CEO/NHNT nanocomposites through solvent casting, presents a schematic depiction of the molecular interactions during the synthesis process. The specific surface area and total pore size of HNT and NHNT were determined using the BET technique. Following NaOH treatment, the internal structure of HNT decomposed and collapsed, increasing the inner diameter of the lumen, and the specific surface area of NHNT increased from 50.16 m^2·g^{-1} of HNT to 57.01 m^2·g^{-1}. The total pore volume increased from 0.25 to 0.32 m^3·g^{-1}, attributed to the removal of Al^{3+} leading to void formation, thereby enhancing the total pore volume of NHNT and improving the adsorption capacity of CEO. TEM results demonstrated that the inner diameter of NHNT exceeded that of HNT. The average inner diameter of NHNT increased to 27 nm, while the wall thickness decreased to 11 nm. This change in inner diameter also resulted in a 30% increase in the outer diameter of NHNT.

The Application Advances of Natural-derived Porous Nanoclays for the Delivery of EOs

Antibacterial agents

Bacterial infectious diseases have caused significant mortality and continue to pose a substantial threat to global human health [157]. The emergence of bacterial resistance has rendered numerous antibiotics ineffective, complicating the treatment of bacterial infections [158]. EOs demonstrate a broad spectrum of antibacterial activity without inducing bacterial resistance, making them a promising therapeutic option for combating bacterial infectious diseases [159, 160]. However, EOs exhibit limitations, such as high volatility, susceptibility to degradation, poor water solubility, and instability when exposed to light and heat [1, 133]. Encapsulating EOs in natural-derived porous nanoclays can enhance their stability while providing sustained release and extending their efficacy duration [61, 127]. This approach represents an effective method to harness the antimicrobial properties of EOs.

Zhang *et al.* [161] developed a novel clay-based topical antibacterial system (TSP) by incorporating tea tree oil (TTO) and salicylic acid (SA) into the natural porous structure of PAL. The antibacterial activity (MIC and MBC) of TSP, TTO-Pal, and SA-Pal against *E. coli*, *S. aureus*, *S. epidermidis*, and *P. acnes* was evaluated. TSP-1 demonstrated the most potent antibacterial activity against all four bacteria, with MIC and MBC values ranging from 10 to 20 g·L^{-1}. The MBC: MIC ratios for TSP-1 against all four bacteria were below 4, indicating a typical bactericidal mechanism. The antibacterial mechanism of TSP-1, which involves disrupting the cell membrane structure, leading to loss of transport function and leakage of cellular contents, ultimately resulting in bacterial death. Pickering emulsification, a novel technology utilizing micro/nano-scale solid particles as emulsifiers, has been reported to employ nanoclays as stabilizers [162, 163]. Hui *et al.* [164] prepared antibacterial Pickering emulsions using *Sapindus mukorossi*-modified palygorskite (*Sm*-Pal) particles as emulsifiers and cinnamaldehyde as the oil phase . The antibacterial efficacy of these emulsions was tested against *E. coli*, *S. aureus*, and two drug-resistant bacteria (ESBL and MRSA). At a concentration of 5 μL·mL^{-1}, the Pickering emulsion achieved reduction rates (R) of 69.8%, 99.6%, 100%, and 99.8% for *Escherichia coli*, *Staphylococcus aureus*, ESBL, and MRSA, respectively, demonstrating excellent antibacterial effects. Complete inhibition (R = 100%) of all four bacteria was achieved at concentrations exceeding 10 μL·mL^{-1}. Moreover, the Pickering emulsification technique enhanced cinnamaldehyde's antibacterial efficacy by increasing the contact probability between the active antibacterial ingredient and bacteria.

Food preservation

Food safety plays a crucial role in safeguarding human

life and health in everyday existence. However, the prevalence of food-related illnesses is on the rise, necessitating the development of safe and environmentally friendly food packaging technologies to ensure food safety and public health [165, 166]. EOs, containing various antibacterial and antioxidant components, are natural food additives derived from plants that have garnered significant attention in the realm of food preservation [167, 168]. Incorporating EOs into safe, nontoxic, and biocompatible natural porous nanoclays to create active food packaging can extend the release duration of EOs active ingredients, thereby achieving long-term antibacterial preservation [29].

CRV, the principal active component in oregano EO, exhibits potent inhibitory effects against various microorganisms, including bacteria, yeasts, and molds [169, 170]. Chakraborty *et al.* [171] encapsulated CR in a composite material comprising HS, banana flour (BF), and glycerol, fabricating BF/HS/CRV bio-composite films through solution casting. The antibacterial efficacy of these films against *Bacillus cereus* and *Escherichia coli* was evaluated using inhibition zone experiments. The results demonstrated that CR-loaded films increased the inhibition zones against *Bacillus cereus* and *Escherichia coli* by 70% and 137%, respectively, compared to the maximum values observed without CRV, indicating CRV's strong antibacterial properties. When applied as a coating on fresh capsicum fruit, the BF/HS/CRV biocomposite film reduced weight loss to 37.42% ± 3.75% and increased hardness to 7.47 ± 0.25 N after 12 days of storage, compared to 50.96% ± 2.40% and 5.04 ± 0.92 N for uncoated fruit. Uncoated capsicum fruit turned completely red by the end of the storage period, while BF/HS/CR coated samples exhibited less redness, demonstrating the biocomposite film's ability to extend shelf life and preserve freshness. Chaudhary *et al*. [172], initially blended CH and HNT to create a CH/HNTs polymer matrix solution. Subsequently, they encapsulated basil EO (BEO) in this matrix through HNT adsorption and ultimately produced a CH/BEO/HNTs nanocomposite film using solution casting. The nanocomposite film containing 15wt% HNT exhibited the highest total phenol content at 88.92 mg GAE·g^{-1}, attributed to the appropriate quantity of HNT particles in the Ch film stabilizing the BEO droplets. 2,2-Diphenyl-1-picrylhydrazyl (DPPH) determination tests also revealed that the nanocomposite film with 15wt% HNT content demonstrated the highest DPPH scavenging activity and strongest antioxidant properties. Furthermore, the nanocomposite film was employed to store broccoli to assess its potential in food packaging applications. Broccoli packaged with the CH/BEO/HNTs nanocomposite film experienced weight loss ranging from 41.07% to 34.34%, substantially lower than the 63.22% weight loss observed in broccoli stored without any film. The morphological changes in broccoli, provide visual evidence of the weight loss variations among broccoli samples packaged in different nanocomposite films. These findings suggest that CH/BEO/HNTs nanocomposite films hold significant potential for applications in the food packaging industry.

Repellent and insecticide

The proliferation of pests during crop growth and grain storage can result in significant economic losses, including crop mortality and grain degradation [173, 174]. While pesticides can effectively control pests to some extent, their prolonged use may lead to pest resistance, environmental contamination, and potential human health risks [175]. Consequently, there is a need for a novel class of pesticides that can meet consumer demands for efficient pest control and food safety. EOs, environmentally friendly natural volatile compounds extracted from aromatic plants, have emerged as a promising solution [176]. Research indicates that EOs and their active components have been utilized as contact insecticides, insect repellents, and fumigants, demonstrating robust insecticidal properties. These properties position EOs as one of the most promising alternatives to conventional insecticides currently available in the market [173, 177]. The incorporation of EOs into natural-derived porous nanoclays facilitates the gradual release of active ingredients from the EOs, thereby providing a sustained insecticidal effect.

Das *et al.* [178] utilized vacuum filtration to incorporate cinnamaldehyde into purified MMT, creating a bio-nanocomposite (CEB) for pest control, employed as a fumigant. The purified MMT's grain size decreased from 6.65 nm to 4.04 nm, while its surface area increased from 33.77 to 77.69 $m^2 \cdot g^{-1}$, enhancing cinnamaldehyde adsorption capacity. Three CEB concentrations (0.08, 0.04, and 0.02 $mg \cdot cm^{-3}$) were tested for repellent activity against *C. chinensis* adults. The higher the concentration of CEB and the longer the treatment time, the stronger the repellent effect. After 6 hours of fumigation treatment with a high concentration (0.08 $mg \cdot cm^{-3}$) of CEB, the repellency rate of *C. chinensis* adults reached 93.33%. This efficacy surpassed the 90% repellency rate reported after a 12-h treatment period in relevant literature [179]. Shaltiel-Harpaz *et al.* [130] developed an insecticidal pesticide using Sepiolite (Sep) as a clay matrix, loaded with *Cinnamomum cassia* EO (CCEO) and rosemary EO (ROEO). CCEO and ROEO were combined with rapeseed oil to assess phytotoxicity on leek seedlings and insecticidal activity against thrips. The results indicated that CCEO had no toxic effect on leek seedlings, while ROEO caused leaf damage even after 50% dilution, rendering it unsuitable for individual use. CCEO demonstrated significant insecticidal effects only at concentrations exceeding 20%, whereas ROEO exhibited potent insecticidal properties with just 1% addition, indicating ROEO's notably strong lethal effect on thrips. Additionally, the study compared the efficacy of raw EOs and clay-based EO composites against thrips. ROEO generally exhibited superior insecticidal activity compared to CCEO. At a CCEO concentration of 350 μL, the thrips mortality rate for CCEO/Sep exceeded 60%, more than double the approximately 30% mortality rate of CCEO alone. Thus, incorporating CCEO into Sep significantly enhanced its lethal impact on thrips. No significant enhancement was observed after load-

ing ROEO into Sep, possibly due to ROEO's inherent strong insecticidal activity. Interestingly, ROEO/Sep reduced the damage of ROEO to leek and mitigated its phytotoxicity. These research findings suggest that using natural-derived porous nanoclays to deliver EOs offers an environmentally friendly, efficient, and durable alternative to conventional insecticides.

Conclusions and Future Perspectives

EOs, as natural bioactive components, offer reduced side effects and enhanced safety compared to synthetic drugs. They demonstrate a broad range of pharmacological activities, including antibacterial, anti-inflammatory, antioxidant, and anthelmintic properties, while also providing psychosomatic regulatory functions such as anxiety reduction. However, their development and application are significantly impeded by poor water solubility, volatile degradation, and thermal instability. Consequently, encapsulation techniques like microencapsulation and the formation of inclusion complexes are frequently employed to protect EOs from volatility and degradation. Nevertheless, these encapsulation methods have specific requirements regarding molecular size and physicochemical properties, limiting their widespread application. In recent years, porous nanocarriers, a category of nanoscale carrier materials with unique pore structures, have attracted increasing attention. This growing interest is attributed to their rapid development, exceptional loading capacity, and the ease with which they can be functionalized.

Natural-derived porous nanoclays serve as effective nanocarriers for EOs due to their abundance, cost-effectiveness, large specific surface area, high porosity, and excellent ion exchange properties. The utilization of these nanoclays for EOs delivery represents an innovative approach. This paper reviews natural-derived porous nanoclays and recent advancements in their application for EOs delivery. Various engineering strategies, including surface modification, particle size control, and activation treatment, are discussed to enhance the efficacy of EOs delivery by these nanoclays. Additionally, the paper explores the applications of natural-derived porous nanoclays in delivering EOs for antibacterial purposes, insect repellency, and food preservation.

Natural-derived porous nanoclays have demonstrated significant potential as delivery carriers for EOs in recent years, with numerous advancements reported in the literature. However, several challenges remain in utilizing these nanoclays as EOs carriers. Firstly, the purity of naturally mined clay minerals is often insufficient, particularly for applications in medicine and drug delivery, where nanoclay safety and biocompatibility are crucial. Secondly, the hydrophilic surface of nanoclays may partially hinder interactions between hydrophobic EOs components and the nanoclay surface. This issue can be mitigated through hydrophobic modification of nanoclays, which can enhance EOs loading capacity. Lastly, while natural-derived porous nanoclays possess high specific surface areas and numerous active groups (such as hydroxyl and silanol groups) on their surfaces, research on nanoclay surface functionalization remains limited. Achieving targeted functionalization of nanoclays or responsive release of EOs could significantly enhance their efficacy in medical applications.

References

[1] Su XY, Lai HZ, Chen SY, *et al*. Raspberry-liked Pickering emulsions based inulin microparticles for enhanced antibacterial performance of essential oils [J]. *Int J Biol Macromol*, 2024, **271**: 132224.

[2] Altay Ö, Köprüalan Ö, İlter I, *et al*. Spray drying encapsulation of essential oils; process efficiency, formulation strategies, and applications [J]. *Crit Rev Food Sci Nutr*, 2024, **64**(4): 1139-1157.

[3] Al-Dhahli AS, Al-Hassani FA, Mohammed Alarjani K, *et al*. Essential oil from the rhizomes of the Saudi and Chinese *Zingiber officinale* cultivars: comparison of chemical composition, antibacterial and molecular docking studies [J]. *J King Saud Univ Sci*, 2020, **32**(8): 3343-3350.

[4] Sousa VI, Parente JF, Marques JF, *et al*. Microencapsulation of essential oils: a review [J]. *Polymers*, 2022, **14**(9): 1730.

[5] Abdi-Moghadam Z, Mazaheri Y, Rezagholizade-shirvan A, *et al*. The significance of essential oils and their antifungal properties in the food industry: a systematic review [J]. *Heliyon*, 2023, **9**(11): e21386.

[6] Lv MY, Sun JB, Wang M , *et al*. Comparative analysis of volatile oils in the stems and roots of *Ephedra sinica via* GC-MS-based plant metabolomics [J]. *Chin J Nat Med*, 2016, **14**(2): 133-140.

[7] De Cicco P, Ercolano G, Sirignano C, *et al*. Chamomile essential oils exert anti-inflammatory effects involving human and murine macrophages: evidence to support a therapeutic action [J]. *J Ethnopharmacol*, 2023, **311**: 116391.

[8] Sharma V, Kumar D, Dev K, *et al*. Anticancer activity of essential oils: cell cycle perspective [J]. *S Afr J Bot*, 2023, **157**: 641-647.

[9] Rajivgandhi G, Kadaikunnan S, Ramachandran G, *et al*. Chitosan loaded plant essential oils efficiently eradicate the multi-drug resistant bacterial infection and lung cancer cells [J]. *J King Saud Univ Sci*, 2023, **35**(5): 102662.

[10] Mohammed HA, Sulaiman GM, Khan RA, *et al*. Essential oils pharmacological activity: chemical markers, biogenesis, plant sources, and commercial products [J]. *Process Biochem*, 2024, **144**: 112-132.

[11] Zhu JL, Jiang XY, Luo XY, *et al*. Discovery and bioassay of disubstituted *β*-elemene-NO donor conjugates: synergistic enhancement in the treatment of leukemia [J]. *Chin J Nat Med*, 2023, **21**(12): 916-926.

[12] Wang L, Fang J, Wang H, *et al*. Natural medicine can substitute antibiotics in animal husbandry: protective effects and mechanisms of rosewood essential oil against *Salmonella* infection [J]. *Chin J Nat Med*, 2024, **22**(9): 1-12.

[13] Bi JP, Li P, Xu XX, *et al*. Anti-rheumatoid arthritic effect of volatile components in notopterygium incisum in rats *via* anti-inflammatory and anti-angiogenic activities [J]. *Chin J Nat Med*, 2018, **16**(12): 926-935.

[14] Sokolik CG, Lellouche JP. Hybrid-silica nanoparticles as a delivery system of the natural biocide carvacrol [J]. *RSC Adv*, 2018, **8**(64): 36712-36721.

[15] Shen C, Li J, Meng Q, *et al*. Rhamnolipids stabilized essential oils microemulsion for antimicrobial and fruit preservation [J]. *Food Chem*, 2024, **457**: 140167.

[16] Vora LK, Gholap AD, Hatvate NT, *et al*. Essential oils for

clinical aromatherapy: a comprehensive review [J]. *J Ethnopharmacol*, 2024, **330**: 118180.
[17] Yang W, Gong YX, Wang YS, *et al*. Design of gum Arabic/gelatin composite microcapsules and their cosmetic applications in encapsulating tea tree essential oil [J]. *RSC Adv*, 2024, **14**(7): 4880-4889.
[18] Da Silva BD, Bernardes PC, Pinheiro PF, *et al*. Chemical composition, extraction sources and action mechanisms of essential oils: natural preservative and limitations of use in meat products [J]. *Meat Sci*, 2021, **176**: 108463.
[19] Liu YM, Li WY, Xu LL, *et al*. Catharmus tinctorius volatile oil promote the migration of mesenchymal stem cells *via* ROCK2/Myosin light chain signaling [J]. *Chin J Nat Med*, 2019, **17**(7): 506-516.
[20] Zafar S, Arshad MF, Khan H, *et al*. Nanoformulations of plant essential oils for managing mycotoxins producing fungi: an overview [J]. *Biocatal Agric Biotechnol*, 2024, **60** : 103314.
[21] Poyatos-Racionero E, Guarí-Borràs G, Ruiz-Rico M, *et al*. Towards the enhancement of essential oil components' antimicrobial activity using new zein protein-gated mesoporous silica microdevices [J]. *Int J Mol Sci*, 2021, **22**(7): 3795.
[22] Lai HZ, Chen SY, Su XY, *et al*. Sponge-liked silica nanoporous particles for sustaining release and long-term antibacterial activity of natural essential oil [J]. *Molecules*, 2023, **28**(2): 594.
[23] Jia JF, Duan SL, Zhou X, *et al*. Long-term antibacterial film nanocomposite incorporated with patchouli essential oil prepared by supercritical CO_2 cyclic impregnation for wound dressing [J]. *Molecules*, 2021, **26**(16): 5005.
[24] Zhou Y, Zhang MJ, Wang CF, *et al*. Solidification of volatile D-Limonene by cyclodextrin metal-organic framework for pulmonary delivery *via* dry powder inhalers: *in vitro* and *in vivo* evaluation [J]. *Int J Mol Sci*, 2021, **606**: 120825.
[25] Caamaño K, Heras-Mozos R, Calbo J, *et al*. Exploiting the redox activity of MIL-100(Fe) carrier enables prolonged carvacrol antimicrobial activity [J]. *ACS Appl Mater Interfaces*, 2022, **14**(8): 10758-10768.
[26] Alinaqi Z, Khezri A, Rezaeinia H. Sustained release modeling of clove essential oil from the structure of starch-based bionanocomposite film reinforced by electrosprayed zein nanoparticles [J]. *Int J Biol Macromol*, 2021, **173**: 193-202.
[27] Majidiyan N, Hadidi M, Azadikhah D, *et al*. Protein complex nanoparticles reinforced with industrial hemp essential oil: characterization and application for shelf-life extension of rainbow trout fillets [J]. *Food Chem X*, 2022, **13**: 100202.
[28] Iravani R, An C, Adamian Y, *et al*. A review on the use of nanoclay adsorbents in environmental pollution control [J]. *Water Air Soil Pollut*, 2022, **233**(4): 109.
[29] Nath D, R S, Pal K, *et al*. Nanoclay-based active food packaging systems: a review [J]. *Food Packag Shelf Life*, 2022, **31**: 100803.
[30] Pereira I, Saleh M, Nunes C, *et al*. Preclinical developments of natural-occurring halloysite clay nanotubes in cancer therapeutics [J]. *Adv Colloid Interface Sci*, 2021, **291**: 102406.
[31] Wang AQ, Wang WB. *1-Introduction. Nanomaterials from clay minerals* [M]. Elsevier. 2019: 1-20.
[32] Lousada ME, Lopez Maldonado EA, Nthunya LN, *et al*. Nanoclays and mineral derivates applied to pesticide water remediation [J]. *J Contam Hydrol*, 2023, **259**: 104264.
[33] Perera M, Jayarathna L, Yakandawala DMD, *et al*. *Nanoclay composites as agrochemical carriers. In*: Vithanage M, Lazzara G, Rajapaksha AU. *Clay composites: environmental applications* [M]. Springer Nature Singapore, 2023: 543-557.
[34] Govea-Alonso DO, García-Soto MJ, Betancourt-Mendiola L, *et al*. Nanoclays: promising materials for vaccinology [J]. *Vaccines*, 2022, **10**(9): 1549.
[35] Fernández MA, Barberia Roque L, Gámez Espinosa E, *et al*. Organo-montmorillonite with biogenic compounds to be applied in antifungal coatings [J]. *Appl Clay Sci*, 2020, **184**: 105369.
[36] Nakhli A, Mbouga MGN, Bergaoui M, *et al*. Modeling of essential oils adsorption onto clays towards a better understanding of their interactions [J]. *J Mol Liq*, 2018, **249**: 132-143.
[37] Pramanik S, Gopalakrishnan R, Barua N, *et al*. Montmorillonite immobilized *Curcuma aromatica*/*Zanthoxylum limonella* oil nanoconjugate as a green antibacterial and biocompatible material with mosquito repellent attributes [J]. *Appl Clay Sci*, 2015, **109-110**: 33-38.
[38] Katti KS, Jasuja H, Jaswandkar SV, *et al*. Nanoclays in medicine: a new frontier of an ancient medical practice [J]. *Mater Adv*, 2022, **3**(20): 7484-7500.
[39] Saadh MJ, Abdulsahib WK, Mustafa AN, *et al*. Recent advances in natural nanoclay for diagnosis and therapy of cancer: a review [J]. *Colloids Surf B Biointerfaces*, 2024, **235**: 113768.
[40] Kashif M, Yuan MH, Su YX, *et al*. A review on pillared clay-based catalysts for low-temperature selective catalytic reduction of NO_x with hydrocarbons [J]. *Appl Clay Sci*, 2023, **233**: 106847.
[41] Das NC, Rahman MM, Kabir SF. Preparation of novel clay/chitosan/ZnO bio-composite as an efficient adsorbent for tannery wastewater treatment [J]. *Int J Biol Macromol*, 2023, **249**: 126136.
[42] Saadat S, Rawtani D, Parikh G. Clay minerals-based drug delivery systems for anti-tuberculosis drugs [J]. *J Drug Deliv Sci Technol*, 2022, **76**: 103755.
[43] Singh NB. Clays and clay minerals in the construction industry [J]. *Minerals*, 2022, **12**(3): 301.
[44] Fareed F, Ibrar M, Ayub Y, *et al*. *Clay-based nanocomposites: potential materials for water treatment applications. In*: Prasad R, Karchiyappan T. *Advanced research in nanosciences for water technology* [M]. Springer International Publishing, 2019: 217-248.
[45] Nomicisio C, Ruggeri M, Bianchi E, *et al*. Natural and synthetic clay minerals in the pharmaceutical and biomedical fields [J]. *Pharmaceutics*, 2023, **15**(5): 1368.
[46] Da Rocha MC, Galdino T, Trigueiro P, *et al*. Clays as vehicles for drug photostability [J]. *Pharmaceutics*, 2022, **14**(4): 796
[47] Gritten Sieben P, Savicki A, Wypych F, *et al*. Oil-in-oil Pickering emulsions stabilized with kaolinite [J]. *J Mol Liq*, 2023, **385**: 122343.
[48] Gianni E, Pšenička M, Macková K, *et al*. New detail insight into halloysite structure: mechanism behind nanotubular morphology described by density functional theory and molecular dynamics supported by experiments [J]. *J Mol Struct*, 2023, **1287**: 135639.
[49] De Oliveira LH, Trigueiro P, Souza JSN, *et al*. Montmorillonite with essential oils as antimicrobial agents, packaging, repellents, and insecticides: an overview [J]. *Colloids Surf B Biointerfaces*, 2022, **209**: 112186.
[50] Wei JY, Li TH, Li F. Synthesis and sonocatalytic performance of $Dy_2Sn_2O_7$/Sepiolite nanocomposite [J]. *J Solid State Chem*, 2023, **328**: 124368.
[51] Lu YS, Wang AQ. From structure evolution of palygorskite to functional material: a review [J]. *Micropor Mesopor Mater*, 2022, **333**: 111765.
[52] Cecilia JA, García-Sancho C, Vilarrasa-García E, *et al*. Synthesis, characterization, uses and applications of porous clays heterostructures: a review [J]. *Chem Rec*, 2018, **18**(7-8): 1085-1104.

[53] Ma YH, Shi CJ, Lei L, *et al*. Research progress on polycarboxylate based superplasticizers with tolerance to clays - a review [J]. *Constr Build Mater.*, 2020, **255**: 119386.
[54] Miranda-Trevino JC, Coles CA. Kaolinite properties, structure and influence of metal retention on pH [J]. *Appl Clay Sci*, 2003, **23**(1): 133-139.
[55] Nicola BP, Bernardo-Gusmão K, Schwanke AJ. *Smectite clay nanoarchitectures: rational design and applications. In*: Kharissova OV, Torres-Martínez LM, Kharisov BI. *Handbook of nanomaterials and nanocomposites for energy and environmental applications* [M]. Springer International Publishing, 2020: 1-32.
[56] Li KK, Li ZY, Men L, *et al*. Potential of ginsenoside Rh2 and its derivatives as anti-cancer agents [J]. *Chin J Nat Med*, 2022, **20**(12): 881-901.
[57] Ross DS, Skyllberg U. *Cation exchange capacity and reactions. In*: Goss MJ, Oliver M. *Encyclopedia of soils in the environment (second edition)* [M]. Elsevier, 2023: 32-42.
[58] Zhu RL, Chen QZ, Zhou Q, *et al*. Adsorbents based on montmorillonite for contaminant removal from water: a review [J]. *Appl Clay Sci*, 2016, **123**: 239-58.
[59] Xie WM, Chen Y, Yang HM. Layered clay minerals in cancer therapy: recent progress and prospects [J]. *Small*, 2023, **19**(34): 2300842.
[60] Wang W, Wu L, Chang L, *et al*. Functionality developments in montmorillonite nanosheet: properties, preparation, and applications [J]. *Chem Eng J*, 2024, **499**: 156186.
[61] Essifi K, Hammani A, Berraaouan D, *et al*. Montmorillonite nanoclay based formulation for controlled and selective release of volatile essential oil compounds [J]. *Mater Chem Phys*, 2022, **277**: 125569.
[62] Saucedo-Zuñiga JN, Sánchez-Valdes S, Ramírez-Vargas E, *et al*. Controlled release of essential oils using laminar nanoclay and porous halloysite/essential oil composites in a multilayer film reservoir [J]. *Micropor Mesopor Mater* , 2021, **316** : 110882 .
[63] Nguemtchouin MGM, Ngassoum MB, Chalier P, *et al*. Ocimum gratissimum essential oil and modified montmorillonite clay, a means of controlling insect pests in stored products [J]. *J Stored Prod Res*, 2013, **52**: 57-62.
[64] Nieto S, Toro N, Robles P, *et al*. Flocculation of clay-based tailings: differences of kaolin and sodium montmorillonite in salt medium [J]. *Materials*, 2022, **15**(3): 1156
[65] Rozhina E, Batasheva S, Miftakhova R, *et al*. Comparative cytotoxicity of kaolinite, halloysite, multiwalled carbon nanotubes and graphene oxide [J]. *Appl Clay Sci*, 2021, **205**: 106041.
[66] Shafei L, Adhikari P, Ching WY. DFT study of electronic structure and optical properties of kaolinite, muscovite, and montmorillonite [J]. *Crystals*, 2021, **11**(6): 618
[67] Brigatti MF, Galán E, Theng BKG. *Chapter 2-structure and mineralogy of clay minerals. Developments in clay science* [M]. Elsevier, 2013, **5**: 21-81.
[68] Siegnin R, Dedzo GK, Ngameni E. Sulfonation of the interlayer surface of kaolinite [J]. *Appl Clay Sci*, 2022, **226**: 106570.
[69] Tournassat C, Bourg IC, Steefel CI, *et al*. *Chapter 1-surface properties of clay minerals. Developments in clay science* [M]. Elsevier, 2015, **6**: 5-31.
[70] Elamathi V, Jayalekshmi S. Quantification of clay minerals and its correlation with chemical and index properties of soil [J]. *Jordan J Civ Eng*, 2023, **17**(1): 163-175.
[71] Awad ME, López-Galindo A, El-Rahmany MM, *et al*. Characterization of Egyptian kaolins for health-care uses [J]. *Appl Clay Sci*, 2017, **135**: 176-189.
[72] Lainé J, Foucaud Y, Hounfodji JW, *et al*. Adsorption of amine surfactants onto kaolinite: a multiscale investigation [J]. *Miner Eng*, 2024, **216**: 108851.
[73] Sidorenko AY, Khalimonyuk TV, Mamatkodirov BD, *et al*. Preparation, acid modification and catalytic activity of kaolinite nanotubes in α-pinene oxide isomerization [J]. *RSC Adv*, 2024, **14**(34): 25079-25092.
[74] Awad ME, López-Galindo A, Setti M, *et al*. Kaolinite in pharmaceutics and biomedicine [J]. *Int J Pharm*, 2017, **533**(1): 34-48.
[75] Mahdi D, Abdellah A. Synergistic antimicrobial activities of limonene with mineral carriers in LDPE films for active packaging application [J]. *Sci J Chem*, 2022, **10**(2): 32-40.
[76] Da Costa RC, Daitx TS, Mauler RS, *et al*. Poly(hydroxybutyrate-co-hydroxyvalerate)-based nanocomposites for antimicrobial active food packaging containing oregano essential oil [J]. *Food Packag Shelf Life*, 2020, **26**: 100602.
[77] Joussein E, Petit S, Churchman J, *et al*. Halloysite clay minerals-a review [J]. *Clay Miner*, 2005, **40**(4): 383-426.
[78] Persano F, Gigli G, Leporatti S. Halloysite-based nanosystems for biomedical applications [J]. *Clays Clay Miner*, 2021, **69**(5): 501-521.
[79] Ouyang J, Mu D, Zhang Y, *et al*. Mineralogy and physicochemical data of two newly discovered halloysite in China and their contrasts with some typical minerals [J]. *Minerals*, 2018, **8**(3): 108.
[80] Maria Calvino M, Cavallaro G, Pasbakhsh P, *et al*. Hydrogel based on patch halloysite nanotubes: a rheological investigation [J]. *J Mol Liq*, 2024, **394**: 123721.
[81] Abdullayev E, Price R, Shchukin D, *et al*. Halloysite tubes as nanocontainers for anticorrosion coating with benzotriazole [J]. *ACS Appl Mater Interfaces*, 2009, **1**(7): 1437-1443.
[82] Fu LJ, Fan DK, Zhang J, *et al*. Microstructure and properties of halloysite nanotubes and modification methods: a comprehensive review [J]. *Appl Clay Sci*, 2024, **253**: 107348.
[83] Ullah A, Sarwar MN, Wang FF, *et al*. *In vitro* biocompatibility, antibacterial activity, and release behavior of halloysite nanotubes loaded with diclofenac sodium salt incorporated in electrospun soy protein isolate/hydroxyethyl cellulose nanofibers [J]. *Curr Res Biotechnol*, 2022, **4**: 445-458.
[84] Lee MH, Seo H-S, Park HJ. Thyme oil encapsulated in halloysite nanotubes for antimicrobial packaging system [J]. *J Food Sci*, 2017, **82**(4): 922-932.
[85] Wang X, Zhu CS, Hu YL, *et al*. Development and application of cinnamaldehyde-loaded halloysite nanotubes for the conservation of stone cultural heritage [J]. *Appl Clay Sci*, 2023, **236**: 106886.
[86] Zheng HM, Mei J, Liu FJ, *et al*. Preparation and characterization of carvacrol essential oil-loaded halloysite nanotubes and their application in antibacterial packaging [J]. *Food Packag Shelf Life*, 2022, **34**: 100972.
[87] Li QQ, Hu XZ, Perkins P, *et al*. Antimicrobial film based on poly(lactic acid) and natural halloysite nanotubes for controlled cinnamaldehyde release [J]. *Int J Biol Macromol*, 2023, **224**: 848-857.
[88] Oliveira PR, Da Costa RC, Malvessi DS, *et al*. Nanocomposites of kaolin modified with oregano essential oil for application in antibacterial packaging [J]. *Appl Clay Sci*, 2023, **241**: 107004.
[89] Wang AQ, Wang WB. *2-Palygorskite nanomaterials: structure, properties, and functional applications. Nanomaterials from clay minerals* [M]. Elsevier, 2019: 21-133.
[90] Wang WB, Wang AQ. Recent progress in dispersion of palygorskite crystal bundles for nanocomposites [J]. *Appl Clay Sci*, 2016, **119**: 18-30.

[91] Guggenheim S, Krekeler MPS. *Chapter 1-the structures and microtextures of the palygorskite–sepiolite group minerals. Developments in clay science* [M]. Elsevier, 2011, **3**: 3-32.
[92] Oliveira KCBF, De Oliveira Farias EA, Teixeira PRS, *et al*. Development of a nanostructured film containing palygorskite and dermaseptin 01 peptide for biotechnological applications [J]. *Clays Clay Miner*, 2023, **71**(5): 600-615.
[93] Ruggeri M, Sánchez-Espejo R, Casula L, *et al*. Bentonite- and palygorskite-based gels for topical drug delivery applications [J]. *Pharmaceutics*, 2023, **15**(4): 1253.
[94] Rusmin R, Sarkar B, Mukhopadhyay R, *et al*. Facile one pot preparation of magnetic chitosan-palygorskite nanocomposite for efficient removal of lead from water [J]. *J Colloid Interface Sci*, 2022, **608**: 575-587.
[95] Lu MY, Qin K, Zhang FY, *et al*. Novel ferrous disulfide loaded palygorskite composites as additives in lignocellulosic waste composting for improving humification [J]. *J Environ Chem Eng*, 2024, **12**(1): 111697.
[96] Ma S, Qian Y, Kawashima S. Performance-based study on the rheological and hardened properties of blended cement mortars incorporating palygorskite clays and carbon nanotubes [J]. *Constr Build Mater*, 2018, **171**: 663-671.
[97] Zhong HQ, Mu B, Zhang MM, *et al*. Preparation of effective carvacrol/attapulgite hybrid antibacterial materials by mechanical milling [J]. *J Porous Mater*, 2020, **27**(3): 843-53.
[98] Lei H, Wei Q, Wang Q, *et al*. Characterization of ginger essential oil/palygorskite composite (GEO-PGS) and its antibacteria activity [J]. *Biomater Adv*, 2017, **73**: 381-387.
[99] Xu CL, Feng YL, Li HR, *et al*. Purification of natural palygorskite clay: process optimization, cleaner production, mineral characterization, and decolorization performance [J]. *Appl Clay Sci*, 2024, **250**: 107268.
[100] Cao LH, Xie WJ, Cui HY, *et al*. Fibrous clays in dermopharmaceutical and cosmetic applications: traditional and emerging perspectives [J]. *Int J Pharm*, 2022, **625**: 122097.
[101] Nie Y, Chen W, Kang Y, *et al*. Two-dimensional porous vermiculite-based nanocatalysts for synergetic catalytic therapy [J]. *Biomaterials*, 2023, **295**: 122031.
[102] Huang RT, Wu LM, Wang XL, *et al*. Review on the effect of isomorphic replacement on the structure and application performance of typical clay minerals [J]. *Prog Nat Sci Mater Int*, 2024, **34**(2): 251-262.
[103] Rumi MK, Urazaeva EM, Nurmatov SR, *et al*. Mineralogical aspects of expanded vermiculite ores [J]. *Glass Ceram*, 2023, **79**(9-10): 386-392.
[104] Zhang Y, Sun HJ, Peng TJ, *et al*. Differential dissolution of interlayer, octahedral and tetrahedral cations of vermiculite in oxalic acid [J]. *Clay Miner*, 2023, **58**(3): 301-309.
[105] Ma L, Huang H, Feng W, *et al*. 2D catalytic, chemodynamic, and ferroptotic vermiculite nanomedicine [J]. *Adv Funct Mater*, 2022, **32**: 2208220.
[106] Li XY, Li RH, Peng K, *et al*. Amine-impregnated porous carbon–silica sheets derived from vermiculite with superior adsorption capability and cyclic stability for CO_2 capture [J]. *Chem Eng J*, 2023, **464**: 142662.
[107] Batista LFA, De Mira PS, De Presbiteris RJB, *et al*. Vermiculite modified with alkylammonium salts: characterization and sorption of ibuprofen and paracetamol [J]. *Chem Pap*, 2021, **75**(8): 4199-4216.
[108] Liu B, He J, Huang K, *et al*. Organic expanded vermiculite as an alternative to filler for improving aging resistance of asphalt mixture [J]. *Case Stud Constr Mat*, 2024, **20**: e03307.
[109] Hou L, Xing BL, Guo H, *et al*. Effect of mineralogical characteristics evolution of vermiculite upon thermal and chemical expansions on its adsorption behavior for aqueous Pb(II) removal [J]. *Powder Technol*, 2023, **430**: 119040.
[110] Wei XC, Liu YN, Zhang Z, *et al*. 2D vermiculite nanofiltration membrane with TiO_2 nanoparticles as versatile intercalator for enhanced water purification [J]. *J Membr. Sci*, 2024, **695**: 122461.
[111] Hu G, Guo D, Shang H, *et al*. Microwave-assisted rapid preparation of vermiculite-loaded nano-nickel oxide as a highly efficient catalyst for acetylene carbonylation to synthesize acrylic acid [J]. *Chemistry Select*, 2020, **5**(10): 2940-2948.
[112] Li XL, Xiao NY, Xiao GS, *et al*. Lemon essential oil/vermiculite encapsulated in electrospun konjac glucomannan-grafted-poly (acrylic acid)/polyvinyl alcohol bacteriostatic pad: sustained control release and its application in food preservation [J]. *Food Chem*, 2021, **348**: 129021.
[113] Kothalawala SG, Zhang J, Wang Y, *et al*. Submicron-sized vermiculite assisted oregano oil for controlled release and long-term bacterial inhibition [J]. *Antibiotics*, 2021, **10**(11): 1324
[114] Shi LP, Qiu JL, Wang W, *et al*. Influence of cations and low molecular weight organic acids on Cs(I) adsorption on montmorillonite and vermiculite [J]. *J Mol Liq*, 2024, **402**: 124778.
[115] Tran YT, Lee J, Kumar P, *et al*. Natural zeolite and its application in concrete composite production [J]. *Compos Part B Eng*, 2019, **165**: 354-364.
[116] Król M. Natural *vs* synthetic zeolites [J]. *Crystals*, 2020, **10**(7): 622
[117] Morante-Carballo F, Montalván-Burbano N, Carrión-Mero P, *et al*. Cation exchange of natural zeolites: worldwide research [J]. *Sustainability*, 2021, **13**(14): 7751
[118] Favvas EP, Tsanaktsidis CG, Sapalidis AA, *et al*. Clinoptilolite, a natural zeolite material: structural characterization and performance evaluation on its dehydration properties of hydrocarbon-based fuels [J]. *Micropor Mesopor Mater*, 2016, **225**: 385-391.
[119] Senila M, Cadar O. Modification of natural zeolites and their applications for heavy metal removal from polluted environments: challenges, recent advances, and perspectives [J]. *Heliyon*, 2024, **10**(3): e25303.
[120] Gorimbo J, Rashama C, Bhondayi C. *Natural zeolites for seawater desalination. Sustainable materials and systems for water desalination* [M]. Springer International Publishing, 2021: 1-14.
[121] Dehmani Y, Ba Mohammed B, Oukhrib R, *et al*. Adsorption of various inorganic and organic pollutants by natural and synthetic zeolites: a critical review [J]. *Arab J Chem*, 2024, **17**(1): 105474.
[122] Feng M, Kou ZR, Tang CY, *et al*. Recent progress in synthesis of zeolite from natural clay [J]. *Appl Clay Sci*, 2023, **243**: 107087.
[123] Kadja GTM, Culsum NTU, Putri RM. Recent advances in the utilization of zeolite-based materials for controlled drug delivery [J]. *Results Chem*, 2023, **5**: 100910.
[124] Ferreira AP, Almeida-Aguiar C, Costa SPG, *et al*. Essential oils encapsulated in zeolite structures as delivery systems (EODS): an overview [J]. *Molecules*, 2022, **27**(23): 8525
[125] Perera AGWU, Karunaratne MMSC, Chinthaka SDM. Prolonged repellent activity of *Ruta graveolens* essential oil adsorbed on different mineral matrices against *Sitophilus zeamais* (L.) (Coleoptera: Curculionidae) [J]. *J Stored Prod Res*, 2022, **97**: 101976.
[126] Migone C, Piras AM, Zambito Y, *et al*. How oregano essential oil can be transformed into a taste-masking controlled release solid formulation [J]. *LWT*, 2024, **201**: 116281.
[127] Milićević Z, Krnjajić S, Stević M, *et al*. Encapsulated clove bud essential oil: a new perspective as an eco-friendly bi-

opesticide [J]. *Agriculture*, 2022, **12**(3): 338
[128] Pires JRA, De Souza VGL, Fernando AL. Chitosan/montmorillonite bionanocomposites incorporated with rosemary and ginger essential oil as packaging for fresh poultry meat [J]. *Food Packag Shelf Life*, 2018, **17**: 142-149.
[129] Biddeci G, Cavallaro G, Di Blasi F, *et al*. Halloysite nanotubes loaded with peppermint essential oil as filler for functional biopolymer film [J]. *Carbohydr Polym*, 2016, **152**: 548-557.
[130] Shaltiel-Harpaz L, Kreimer T, Dudai N, *et al*. Sepiolite- rosemary oil combination as an environmentally oriented insecticide [J]. *Appl Clay Sci*, 2023, **234**: 106838.
[131] Aghajani-Memar S, Hamedi S, Kermanian H. Preparation of the edible fragrant antibacterial sodium caseinate–based nanocomposite containing rosa damascena essential oil and halloysite nanotube [J]. *Food Bioproc Tech*, 2024, **17**(9): 2885-2901.
[132] Zhang X, Cao LH, Li HY, *et al*. Construction of tea tree oil/salicylic acid/palygorskite hybrids for advanced antibacterial and anti-inflammatory performance [J]. *J Mater Chem B*, 2023, **11**(19): 4260-4273.
[133] Ye ZW, Yang QY, Lin QH, *et al*. Progress of nanopreparation technology applied to volatile oil drug delivery systems [J]. *Heliyon*, 2024, **10**(2): e24302.
[134] Zhang Y, Long Y, Yu S, *et al*. Natural volatile oils derived from herbal medicines: a promising therapy way for treating depressive disorder [J]. *Pharmacol Res*, 2021, **164**: 105376.
[135] Su XY, Li B, Chen SY, *et al*. Pore engineering of micro/mesoporous nanomaterials for encapsulation, controlled release and variegated applications of essential oils [J]. *J Control Release*, 2024, **367**: 107-134.
[136] Dong JN, Cheng ZN, Tan SW, *et al*. Clay nanoparticles as pharmaceutical carriers in drug delivery systems [J]. *Expert Opin Drug Deliv*, 2021, **18**(6): 695-714.
[137] Wan HA, Liu DD, Shao LS, *et al*. Simple and scalable preparation of lignin based porous carbon coated nano-clay composites and their efficient removal for the diversified iodine [J]. *Int J Biol Macromol*, 2024, **270**: 132091.
[138] Wang WB, Wang AQ. *Nanoscale clay minerals for functional ecomaterials: fabrication, applications, and future trends. In*: Martínez LMT, Kharissova OV, Kharisov BI. *Handbook of ecomaterials* [M]. Springer International Publishing, 2019: 2409−2490.
[139] Arabmofrad S, Jafari SM, Lazzara G, *et al*. Preparation and characterization of surface-modified montmorillonite by cationic surfactants for adsorption purposes [J]. *J Therm Anal Calorim*, 2023, **148**(24): 13803-13814.
[140] Chu YT, Dai Y, Xia MZ, *et al*. The enhanced adsorption of diclofenac sodium (DCF) and ibuprofen (IBU) on modified montmorillonite with benzyldimethylhexadecylammonium chloride (HDBAC) [J]. *Colloids Surf A Physicochem Eng Aspects*, 2024, **681**: 132764.
[141] De Barros A, Ferreira M, Constantino CJL, *et al*. Nanocomposites based on LbL films of polyaniline and sodium montmorillonite clay [J]. *Synth Met*, 2014, **197**: 119-125.
[142] Sirajunnisa P, Sreelakshmi S, Sailaja GS. Lawsonia inermis-organically modified chitosan intercalated bentonite clay: a multifunctional nanotheranostic system for controlled drug delivery, sensing and cellular imaging [J]. *Int J Biol Macromol*, 2024, **262**: 130209.
[143] Taş CE, Gundogdu SO, Ünal H. Polydopamine-coated halloysite nanotubes for sunlight-triggered release of active substances [J]. *ACS Appl Nano Mater*, 2022, **5**(4): 5407-5415.
[144] Li ZP, Yan HJ, Zhang FQ. Hydrophobicity of montmorillonite synergistically controlled by silanization and aliphatic amine modification [J]. *Colloids Surf A Physicochem Eng Aspects*, 2024, **694**: 134185.
[145] Luo DY, Wei JQ. Efficacy of functionalized sodium-montmorillonite in mitigating alkali-silica reaction [J]. *Appl Clay Sci*, 2023, **245**: 107139.
[146] Sabre EV, Casuscelli SG, Cánepa AL, *et al*. Vanadium-containing modified clays as catalysts for acetaldehyde production by ethanol selective oxidation [J]. *Catal Today*, 2024, **442**: 114911.
[147] Proença LB, Righetto GM, Camargo ILBdC, *et al*. Poly(acid lactic)-montmorillonite clay bionanocomposites loaded with tea tree oil for application in antibacterial wound healing [J]. *Hybrid Adv*, 2024, **6**: 100201.
[148] Liu P. Polymer modified clay minerals: a review [J]. *Appl Clay Sci*, 2007, **38**(1): 64-76.
[149] Upasani AA, Hirpara YS, Gogate PR. Ultrasound-assisted particle size reduction of palygorskite clay [J]. *Chem Pap*, 2024, **78**(2): 779-792.
[150] Xu J, Wang WB, Lu YS, *et al*. Ultrasonic disaggregation of dioctahedral palygorskite crystal bundles for enhancing the stability and antibacterial properties of Pickering emulsion [J]. *Appl Clay Sci*, 2023, **238**: 106933.
[151] Low LE, Siva SP, Ho YK, *et al*. Recent advances of characterization techniques for the formation, physical properties and stability of Pickering emulsion [J]. *Adv Colloid Interface Sci*, 2020, **277**: 102117.
[152] Worasith N, Goodman BA. Clay mineral products for improving environmental quality [J]. *Appl Clay Sci*, 2023, **242**: 106980.
[153] Alanazi AM, Jefri OA, Alam MG, *et al*. Organo acid-activated clays for water treatment as removal agent of Eosin-Y: Properties, regeneration, and single batch design absorber [J]. *Heliyon*, 2024, **10**(10): e30530.
[154] Fashtali AR, Payan M, Zanganeh Ranjbar P, *et al*. Attenuation of Zn (II) and Cu (II) by low-alkali activated clay-fly ash liners [J]. *Appl Clay Sci*, 2024, **250**: 107298.
[155] Marsh ATM, Krishnan S, Bernal SA. Structural features of thermally or mechano-chemically treated montmorillonite clays as precursors for alkali-activated cements production [J]. *Cem Concr Res*, 2024, **181**: 107546.
[156] Boro U, Priyadarsini A, Moholkar VS. Synthesis and characterization of poly (lactic acid)/clove essential oil/alkali-treated halloysite nanotubes composite films for food packaging applications [J]. *Int J Biol Macromol*, 2022, **216**: 927-939.
[157] You YH, Sun H, Cheng ZY, *et al*. Advanced stimuli-responsive host-guest biomaterials for treating bacterial infections [J]. *Polymer*, 2024, **307**: 127312.
[158] Tageldin A, Omolo CA, Nyandoro VO, *et al*. Engineering dynamic covalent bond-based nanosystems for delivery of antimicrobials against bacterial infections [J]. *J Control Release*, 2024, **371**: 237-257.
[159] Chen SY, Lai HZ, Su XY, *et al*. Rambutan-liked Pickering emulsion stabilized by cellulose nanocrystals for enhancing anti-bacterial activity and anti-inflammatory effect of *Chimonanthus nitens Oliv.* essential oil [J]. *Int J Biol Macromol*, 2023, **242**: 124665.
[160] Yuan CX, Hao XQ. Antibacterial mechanism of action and in silico molecular docking studies of *Cupressus funebris* essential oil against drug resistant bacterial strains [J]. *Heliyon*, 2023, **9**(8): e18742.
[161] Zhang Y, Tang LD, Wang JY, *et al*. Anti-inflammatory effects of aucubin in cellular and animal models of rheumatoid arthritis [J]. *Chin J Nat Med*, 2022, **20**(6): 458-472.
[162] Lu TT, Gou H, Rao HH, *et al*. Recent progress in nanoclay-based Pickering emulsion and applications [J]. *J Environ*

Chem Eng, 2021, **9**(5): 105941.
[163] Wang SJ, Shen Y, Chen XP, *et al*. Cationic surfactant-modified palygorskite particles as effective stabilizer for Pickering emulsion gel formation [J]. *Appl Clay Sci*, 2022, **219**: 106439.
[164] Hui AP, Duan FZ, Zhu YF, *et al*. Sapindus mukorossi modified palygorskite particles for stabilizing Pickering emulsions and enhancing antibacterial activities [J]. *Colloid Interface Sci Commun*, 2023, **53**: 100702.
[165] Geng LJ, Huang JC, Fang MX, *et al*. Recent progress of the research of metal-organic frameworks-molecularly imprinted polymers (MOFs-MIPs) in food safety detection field [J]. *Food Chem*, 2024, **458**: 140330.
[166] Qi S, Hamed EM, Ma P, *et al*. Perovskite nanocrystals (PNCs) served as an emerging optical indicator for food safety and quality assessment: progress, challenges, and opportunities [J]. *Coord Chem Rev*, 2024, **514**: 215925.
[167] Ru YB, Zhu YQ, Wang X, *et al*. Edible antimicrobial yeast-based coating with basil essential oil for enhanced food safety [J]. *Innov Food Sci Emerg Technol*, 2024, **93**: 103612.
[168] Li ZY, Yang C, Li ZY, *et al*. Application and safety evaluation of an anti-aflatoxigenic chitosan pouch containing turmeric essential oil in the storage of traditional Chinese health food [J]. *Int J Biol Macromol*, 2021, **183**: 1948-1958.
[169] Duan WY, Zhu XM, Zhang SB, *et al*. Antifungal effects of carvacrol, the main volatile compound in *Origanum vulgare* L. essential oil, against *Aspergillus flavus* in postharvest wheat [J]. *Int J Food Microbiol*, 2024, **410**: 110514.
[170] Rathod NB, Kulawik P, Ozogul F, *et al*. Biological activity of plant-based carvacrol and thymol and their impact on human health and food quality [J]. *Trends Food Sci Tech*, 2021, **116**: 733-748.
[171] Chakraborty P, Hati S, Mishra BK. Biocomposite films from banana flour/halloysite nanoclay/carvacrol: preparation, characterization, and application on capsicum (*Capsicum annuum*) fruits [J]. *Sustain Chem Pharm*, 2023, **36**: 101304.
[172] Chaudhary N, Mishra G, Yadav T, *et al*. Fabrication and evaluation of basil essential oil-loaded halloysite nanotubes in chitosan nanocomposite film and its application in food packaging [J]. *Antibiotics*, 2022, **11**(12): 1820
[173] Rajkumar V, Gunasekaran C, Paul CA, *et al*. Development of encapsulated peppermint essential oil in chitosan nanoparticles: characterization and biological efficacy against stored-grain pest control [J]. *Pestic Biochem Phys*, 2020, **170**: 104679.
[174] Elumalai K, Krishnappa K, Pandiyan J, *et al*. Characterization of secondary metabolites from Lamiaceae plant leaf essential oil: a novel perspective to combat medical and agricultural pests [J]. *Physiol Mol Plant Pathol*, 2022, **117**: 101752.
[175] Mattar VT, Borioni JL, Hollman A, *et al*. Insecticidal action, repellency, and toxicity mechanism of the essential oil of *Lippia turbinata* against the stored product pest *Rhipibruchus picturatus* (F.) [J]. *Pestic Biochem Phys*, 2024, **201**: 105907.
[176] Alves MdS, Campos IM, Brito DdMCd, *et al*. Efficacy of lemongrass essential oil and citral in controlling *Callosobruchus maculatus* (Coleoptera: Chrysomelidae), a post-harvest cowpea insect pest [J]. *Crop Prot*, 2019, **119**: 191-196.
[177] Ma SJ, Jia R, Guo ML, *et al*. Insecticidal activity of essential oil from *Cephalotaxus sinensis* and its main components against various agricultural pests [J]. *Ind Crops Prod*, 2020, **150**: 112403.
[178] Das R, Borthakur S, Arokiyaraj C, *et al*. A novel montmorillonite clay based bio-nanocomposite as an emerging biocontrol agent against stored grain pulse beetle [J]. *Hybrid Adv*, 2024, **5**: 100138.
[179] Wei JY, Shi WW, Zhao T, *et al*. Sustained release and insect repellent activity of cinnamon essential oil active label based on three-step encapsulating [J]. *Food Biosci*, 2023, **56**: 103165.

Cite this article as: CHEN Hongxin, SU Xiaoyu, LUO Yijuan, *et al*. Natural-derived porous nanocarriers for the delivery of essential oils [J]. *Chin J Nat Med*, 2024, **22**(12): 1117-1133.